

see commentary on page 479

The normal kidney filters nephrotic levels of albumin retrieved by proximal tubule cells: Retrieval is disrupted in nephrotic states

LM Russo¹, RM Sandoval², M McKee¹, TM Osicka³, AB Collins⁴, D Brown¹, BA Molitoris^{2,5} and WD Comper³

¹Program in Membrane Biology, Renal Unit, Massachusetts General Hospital and Harvard Medical School, Boston, Massachusetts, USA;

²Division of Nephrology, Department of Medicine and the Indiana Center for Biological Microscopy, Indiana University School of Medicine, Indianapolis, Indiana, USA; ³Department of Medicine, University of Melbourne, Austin Health, Heidelberg, Victoria, Australia;

⁴Pathology Unit, Massachusetts General Hospital and Harvard Medical School, Boston, Massachusetts, USA and ⁵The Roudebush Veterans Administration Medical Center, Indianapolis, Indiana, USA

The origin of albuminuria remains controversial owing to difficulties in quantifying the actual amount of albumin filtered by the kidney. Here we use fluorescently labeled albumin, together with the powerful technique of intravital 2-photon microscopy to show that renal albumin filtration in non-proteinuric rats is ~50 times greater than previously measured and is followed by rapid endocytosis into proximal tubule cells (PTCs). The endocytosed albumin appears to undergo transcytosis in large vesicles (500 nm in diameter), identified by immunogold staining of endogenous albumin by electron microscopy, to the basolateral membrane where the albumin is disgorged back to the peritubular blood supply. In nephrotic rats, the rate of uptake of albumin by the proximal tubule (PT) is decreased. This is consistent with reduced expression of clathrin, megalin, and vacuolar H⁺-ATPase A subunit, proteins that are critical components of the PT endocytotic machinery. These findings strongly support the paradigm-shifting concept that the glomerular filter normally leaks albumin at nephrotic levels. Albuminuria does not occur as this filtered albumin load is avidly bound and retrieved by PTCs. Dysfunction of this retrieval pathway leads to albuminuria. Thus, restoration of the defective endocytotic and processing function of PT epithelial cells might represent an effective strategy to limit urinary albumin loss, at least in some types of nephrotic syndrome.

Kidney International (2007) **71**, 504–513. doi:10.1038/sj.ki.5002041; published online 17 January 2007

KEYWORDS: albuminuria; proximal tubule; glomerular filtration barrier; nephropathy; pathophysiology of renal disease and progression

Correspondence: WD Comper, Department of Medicine, University of Melbourne, Austin Health, Heidelberg, Victoria 3084, Australia.
E-mail: wcomper@hotmail.com

Received 1 May 2006; revised 2 October 2006; accepted 1 November 2006; published online 17 January 2007

The major barrier to the passage of albumin into the urine has long been thought to reside in the glomerular capillary wall, partly on the basis of massive proteinuria associated with genetic diseases of the glomerular epithelial cell (podocyte)¹ and the very low concentrations of albumin measured in the filtered fluid by micropuncture methods² in the early tubular lumen. The restrictive permselectivity of the glomerular filter to albumin has been attributed to exclusion of albumin based on its size and in particular its electrical charge. However, recent studies have shown that electrical repulsion of anionic polysaccharides by the glomerular capillary wall could not account for the apparent low permselectivity of albumin.^{3–8}

In order to directly measure albumin filtration, we have used the minimally invasive, non-toxic technique of intravital 2-photon microscopy which allows a four-dimensional (volume and time) examination of physiological processes in the kidney.⁹ This technique has previously been used to demonstrate subcellular trafficking and transcytosis in proximal tubular cells (PTCs)¹⁰ as well as determining the glomerular sieving of different molecular weight dextrans.⁸ Here we evaluate the second to second dynamics of albumin filtration and cellular uptake *in vivo* in normal and nephrotic rats using fluorescent-labeled albumin. Electron microscopy was used to identify intracellular transport of endogenous albumin. Further, we use immunocytochemistry to determine changes in critical components of the proximal tubule (PT) endocytic machinery including expression of the albumin receptor megalin, vacuolar H⁺-ATPase A subunit (v-ATPase) and clathrin in nephrotic rats.

These data provide fundamental new insights into the extent of albumin filtration by the kidney and the critical role of post-glomerular albumin reabsorption in the prevention of nephrotic levels of albuminuria.

RESULTS

Rapid filtration of albumin

Studies were undertaken to examine whether albumin could be visualized in the post-glomerular space (Bowman's space) or in association with PTCs using 2-photon microscopy. Figure 1a shows the S1 segment leading directly from the Bowman's capsule containing the glomerular capillary loops in a Munich–Wistar rat. Fluorescent rat serum albumin (Alexa 488-RSA (green)) was introduced by a small bolus intravenous injection into the femoral vein, and rapidly appeared as a bright band along the brush border of the PT within 7 s (Figure 1a, see also Movie S1). Over time it appeared to bind further down the S1 segment of the PT as seen in Figure 1b.

The high capacity processing of albumin could be seen on the brush border. The enrichment of albumin on the brush border in the concentration range of 1–10 mg/ml (estimated using a line tool and standard curve for fluorescent intensity as described in Materials and Methods) was consistently observed for different fluorescent albumins and in different rat strains. Femoral injection of free Alexa 568 dye resulted in no significant enrichment on the brush border, and the dye was rapidly cleared (~2 min) from the circulation (data not shown).

Analysis of the GSC of albumin

For bolus femoral injections of Alexa 568-RSA (red), measurements in eight different glomeruli/S1 units from eight animals gave glomerular sieving coefficient (GSC) values of 0.0341 ± 0.0095 (s.d.) ($n=28$) from 30 s up to 30 min. Table 1 shows the details of the variation in plasma

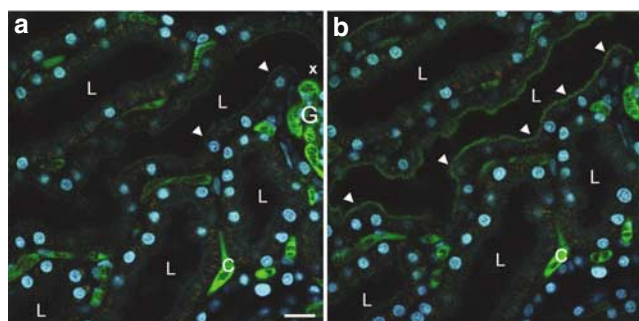


Figure 1 | Rapid binding and accumulation of albumin on the brush border. (a) Image taken 10 s following the appearance of Alexa 488-RSA in the glomerular capillaries (initially seen 7 s total following femoral vein injection). Albumin is seen bound to the brush border (arrows) in the immediate S1 segment leading from the glomerulus (G). C – capillary and L – tubular lumen. In other experiments albumin could be seen bound to the brush border in as little as 2 s following the appearance of albumin in the glomerular capillaries. The nuclei (blue) are labeled with Hoechst 33342. The position denoted 'X' marks the center of the interface of the S1 tubular lumen with the Bowman's capsule where estimates of the GSC were made. (b) Image taken at 90 s following femoral injection of Alexa 488-RSA. Albumin is clearly seen binding to the brush border along the tubular lumen leading from the glomerulus in the upper right hand corner. Bar = 25 μ m. See Movie S1.

and Bowman's capsule fluorescence as a function of time. The time independence of GSC for bolus injections demonstrates that albumin filtration is associated with a steady-state convective flux not influenced by time-dependent diffusion, hemodynamic effects associated with the introduction of the fluorescent albumin, or anomalous low-molecular weight contaminants in the fluorescent albumin preparation.

Results for non-saturating steady-state levels of plasma fluorescence where glomerular capillary fluorescence is measured directly are shown in Table 2. The GSC values for fluorescein isothiocyanate-inulin were close to 1 as expected. Values for the GSC for albumin were in the range of 0.02–0.04 and time independent over 30 min. The GSC values were independent of the concentration of fluorescent albumin in plasma (including both non-steady-state and steady-state experiments the concentration varied by a factor ~10). Overall, the GSC values are far higher than that obtained from micropuncture of 0.0006.²

Post-glomerular processing of albumin and other macromolecules

Nagase analbuminemic rats lack plasma albumin thus any competition for the filtration and uptake with endogenous albumin is diminished resulting in a higher fluorescent ratio. Their kidneys process exogenous albumin in exactly the same manner as Munich–Wistar or Sprague–Dawley rats.¹¹ Figure 2a shows a silhouette of the brush border extending far into the tubular lumen, whereas fluorescent albumin localization was prominent only at the base of the brush border (Figure 2b) (see Movie S2). Similar findings were seen in Munich–Wistar rats (see Movie S3).

Upon further analysis of the levels of albumin bound to the brush border using fluorescence intensity linescans at two different areas of interest (aoi) (Figure 2b), finite changes in albumin concentration were noted not only on the brush border but also intracellularly in the PTC and in the tubular lumen. Importantly, the changes in the intracellular levels of albumin were similar to those observed in the lumen suggesting that there may be a constant flow of albumin across the cell membrane.

Table 1 | Examples of GSC estimated in non-steady-state saturating levels of plasma albumin fluorescence

Time	Plasma fluorescence		Bowman's space		GSC	
	1:15 dilution		Rat 1	Rat 2	Rat 1	Rat 2
	Rat 1	Rat 2				
15 s	20	21				
25 s			29	13		
1 min			29	13		
2.3 min	50	19	29	13	0.039	0.043
5.5 min	46	19	24	11	0.035	0.039
10 min	45	21	25	9	0.031	0.029
15 min	43	21	21	9	0.033	0.029

GSC, glomerular sieving coefficient.

Rat 1 injected with an initial bolus of 400 μ l whereas rat 2 with an initial bolus of 200 μ l.

Variation as observed in two individual nephrons over time.

Table 2 | GSCs estimated at non-saturating, steady-state levels of plasma fluorescence

Rat	Glomerular capillary loop fluorescence units				Bowman's space fluorescence units				GSC						
	1	2	3	4	1	2	3	4	1	2	3	4			
<i>Fluorescent inulin</i>															
Time (min)															
5	155	145	73	130	157	150	75	136	1.01	1.03	1.03	1.05			
7	101				115				1.14						
10	175	180	159	174	187	186	166	180	1.07	1.03	1.04	1.03			
12	137	186	163	194	140	192	173	201	1.02	1.03	1.06	1.04			
15	131	184	154	195	139	196	162	201	1.06	1.07	1.05	1.03			
20	143	187	166	189	151	195	180	203	1.06	1.04	1.08	1.07			
Rat	Glomerular capillary loop fluorescence units					Bowman's space fluorescence units					GSC				
	1	2	3	4	5	1	2	3	4	5	1	2	3	4	5
<i>Fluorescent albumin</i>															
Time (min)															
5	62	100	183	183	137	3	2	7	5	3	0.048	0.020	0.038	0.027	0.022
10	63	97	179	185	139	3	2	7	5	3	0.047	0.021	0.039	0.027	0.022
13	66					2					0.030				
15	59	94	165	189	141	2	2	6	5	3	0.034	0.021	0.036	0.026	0.021
17		73					2					0.027			
20	56		177	186	151	2		7	5	3	0.036		0.040	0.027	0.020
21		83					2					0.024			
25			170	181	154			7	5	3			0.041	0.028	0.019
30			200	185	146			8	5	3			0.040	0.027	0.021

GSC, glomerular sieving coefficient.

Over relatively longer periods we observed that some of the internalized fluorescent albumin appeared in large intracellular vesicular structures that were often arranged in a longitudinal 'striated' pattern (Figure 3). The formation of these structures is rapid and dynamic (see Movie S4). After 43 min these striations extend from the apical to the basolateral side of the PTC (Figure 3b) and some remained detectable even 24 h post-infusion (Figure 3c).

Electron microscopical analysis of endogenous albumin in PTCs revealed the presence of large vesicles (diameter ~500 nm) containing large quantities of gold-labeled albumin (Figure 4). These vesicles are similar in size to those seen by 2-photon fluorescence microscopy (Figure 3 and Movie S4). As the albumin antibodies used here do not detect the albumin fragments generated by lysosomes,³ this result indicates that large amounts of intact albumin are present in these vesicles. The vesicles were distributed throughout the cell, and often lined up within the slender basolateral cytoplasmic fingers formed by membrane invaginations in PTCs in the S1 segment, producing the 'striated' appearance that was seen by fluorescence microscopy. Finally and critically, many of these large vesicles were seen in close proximity to the basolateral plasma membrane. Images of vesicle fusion with this membrane domain were readily detectable and their albumin-rich content was clearly visualized discharging into the peritubular space adjacent to capillaries (Figure 4).

Albumin uptake in nephrotic states

The nephrotic state was induced in rats by the administration of puromycin aminonucleoside. The albumin excretion rate

in puromycin aminonucleoside nephrosis (PAN) rats is >300 mg/day.^{12,13} As the PAN rat is hypoalbuminemic (plasma concentration is reduced by two-thirds),¹³ the concentration of fluorescent-labeled albumin was adjusted (also reduced by two-thirds) so that the ratio of labeled albumin to unlabeled endogenous albumin was essentially the same for untreated control rats and PAN rats. It is apparent that ~40 s after the initial bolus there was little or no uptake of albumin by the brush border of PTCs from PAN rats compared to non-treated rats even though there were significant quantities present in the tubular lumen of both proximal and distal tubules (Figure 5). Even after 14 min the fluorescent albumin binding to the brush border of PTCs in PAN rats appeared patchy (see Movies S5 and S6).

The corresponding images of the untreated control and PAN rats are also shown in pseudocolor in Figure 6. Pseudocolor converts varying levels of fluorescent intensity into a color spectrum. Autofluorescence indicative of PTs can be seen in both the pre-injected control and PAN rats (Figure 6a and d). Differences in the autofluorescence may reflect differences associated with individual rats and the PAN state. The low levels of filtered fluorescent albumin are seen as a magenta color. In the control rat, a magenta haze was apparent in the tubular lumen as well as in the cytoplasm of the PTCs (Figure 6b and c). The image featured by the arrow reflects increasing resident albumin concentrations moving from yellow (Figure 6a) to magenta (Figure 6b) to light green/turquoise (Figure 6c). In contrast, there was significantly more fluorescent albumin in the tubular lumen but considerably reduced quantities of fluorescent albumin appearing as a haze in the cytoplasm in PAN rats; areas near

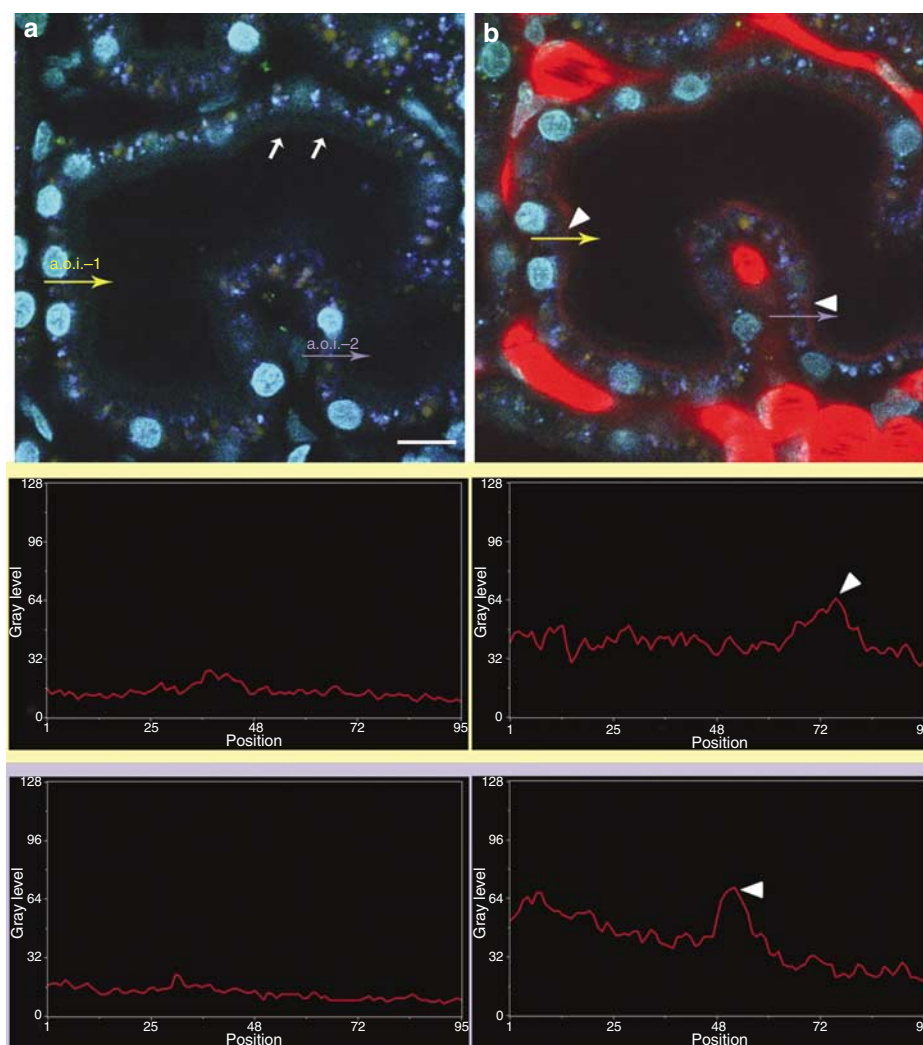


Figure 2 | Albumin binding is localized to the base of the brush border. Images shown in (a) are from nagase analbuminemic rats at pre-injection and (b) 90 s after femoral injection of Alexa 568-RSA. The nuclei (blue) are labeled with Hoechst 33342. Anionic cascade blue dextran (1.6 mg in normal saline) molecular weight 3000 was given approximately 15 min before femoral injection of albumin. White arrows indicate silhouette of the brush border that is present in a. Albumin uptake appears as a band on the base of the brush border visible in b. Graphs representing line-scans across cells (obtained in the red channel) are shown below the microscopical images for two aoi (yellow aoi-1 and purple aoi-2). In aoi-1 in b, the brush border is seen as the major peak together with significantly elevated levels of Alexa 568-RSA both inside the cell and in the tubular lumen as compared to the low background levels seen in line-scans from a of the pre-injected rat. (Pixels run from left to right in direction of colored arrows (basal to apical to tubular lumen). The white arrowheads feature the albumin-binding region. Similar features can be seen for aoi-2. Bar = 15 μ m. See Movie S2.

the arrow appeared yellow (Figure 6d), yellow (Figures 6e) and magenta/yellow (Figure 6f). Therefore, in the PAN condition there is significant inhibition of the tubular uptake of albumin by the brush border of PTCs.

Changes in apical endocytotic machinery as a mechanism of albuminuria

In tissue from nephrotic rats, there was a dramatic decrease in the expression of megalin, v-ATPase, and clathrin in the apical pole of the PT (Figure 7) (images are shown in Figure S1) relative to control tissue. These proteins are key players in the apical endocytotic machinery in PT epithelial cells and this observation is consistent with the reduction in albumin

endocytosis observed in the PAN rats by 2-photon microscopy (Figures 5 and 6).

DISCUSSION

A major finding of this study is that the GSC for fluorescently labeled albumin, when measured in non-proteinuric rats, is 0.034 which is much higher than previously reported. The GSC for albumin is similar for both bolus injection experiments and steady-state infusion experiments. The time independence of the GSC is clear evidence that the nephron is functioning normally with dominant filtration or convective flow over that of diffusion (which may occur at lower glomerular filtration rates). Further, analysis of inulin

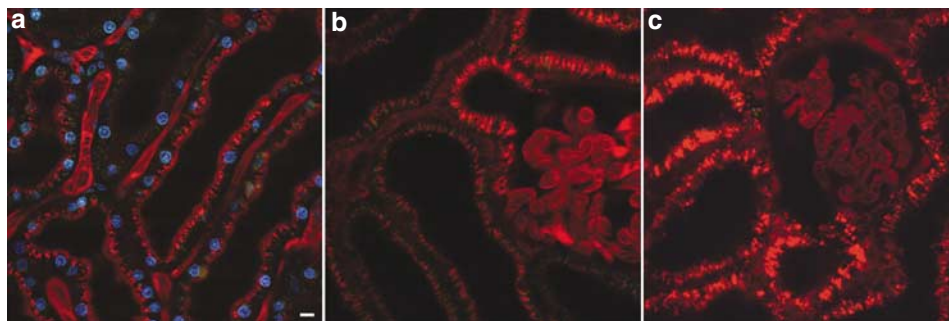


Figure 3 | Short- and long-term vesicular localization of labeled albumin. (a) Localization of Alexa 568-RSA after 12 min post-injection in Munich-Wistar rats. Large vesicles containing the fluorescent-labeled material are present throughout the cytoplasm. (b) Localization at 43 min and (c) 24 h accumulation of fluorescent material in the PTC; note the presence of Alexa 568-RSA in the glomerular capillaries. Bar = 10 μm .

clearance using the same technique as that used for the albumin returned values of ~ 1.0 , consistent with that predicted and previously measured for inulin which is not processed by PTCs. The fact that the fluorescent albumin has a normal and prolonged plasma elimination rate *in vivo* (see Materials and Methods) and a normal fractional clearance in the isolated perfused kidney (see Materials and Methods) suggests that filtered albumin must be reabsorbed back to the blood most likely via retrieval by the PT.

Evidence in favor of the existence of a retrieval pathway for intact albumin in PTCs *in situ* comes from our electron microscopical observations using immunogold staining for intact albumin. Many cytoplasmic vesicles contained large quantities of albumin, and these vesicles appear to fuse with the basolateral plasma membrane, resulting in the release of albumin into the peritubular capillary. This is correlated with the presence of linear structures, seen by 2-photon microscopy, that contain albumin and that extend from the apical to the basolateral side of the PTCs over time. These linear structures probably represent rows of albumin containing vesicles confined within the narrow cytoplasmic basolateral extensions that are present in some regions of the PT, notably the S1 segment. In support of these morphological observations, filtered albumin has been demonstrated to be returned to the renal vein¹⁴ and transcytosis of albumin may be inferred from measurements in cultured PTCs.¹⁵

The high GSC for albumin of 0.034 is consistent with a number of other studies. It is close to the value predicted for the filtration of intact albumin controlled by size selectivity alone without influence of charge selectivity.¹⁶ The GSC is also similar in value to (i) the fractional clearance of albumin where the proximal tubular cell uptake has been inhibited through the use of toxins,¹⁷ (ii) mildly denatured albumin that has the same charge and size as native albumin but is conformationally altered consistent with its inability to be recognized by the retrieval pathway PTC receptor,¹⁸ (iii) fractional clearance of albumin in overload albuminuria where the retrieval pathway is approaching saturation,¹⁹ and (iv) fractional clearance of albumin in various nephrotic states where PTC uptake is probably inhibited.^{20,21} The high

GSC is also consistent with capillary wall sieving coefficients of albumin in non-renal fenestrated capillaries.²⁰

The observations made in this study and elsewhere delineate two pathways of albumin processing in the PTC. The albumin binds and is enriched at the base of the PT brush border. Binding of albumin to the brush border has been observed previously²² but our 2-photon studies which enable live non-invasive imaging now demonstrate that it is a rapid and high capacity binding. The enrichment of albumin on the brush border is typical of a receptor-mediated process, as compared to fluid phase endocytosis, and may involve association with megalin/cubilin receptors^{23–25} or other receptors that are located in PT apical membranes. From this region, albumin is either rapidly processed by a high capacity pathway involving transcytosis that has also been previously proposed^{13,14,17,19} or a lower capacity pathway directed towards lysosomal delivery and degradation.^{3,11,17,20,26} This is consistent with the fact that in control rats we do not observe albuminuria, although the levels of albumin being filtered would, if not processed by PTCs, give rise to albumin excretion rates similar to that seen in nephrotic conditions. The involvement of this pathway in albumin uptake and its perturbation in the nephrotic condition is supported by our present observations that the membrane expression of key proteins of the apical endocytotic machinery²⁷ (megalin, the V-ATPase, and clathrin) is greatly reduced in PAN-treated animals.

The high GSC means that albumin is normally filtered at a rate of ~ 2 g/rat/day (in rats the GSC corresponds to a flux of albumin across the glomerulus of 29 ng/min assuming single nephron glomerular filtration rate of 30 nl/min and a plasma albumin of 30 mg/ml). Overall, the kidney would be filtering ~ 1.2 g albumin/kidney/day (assuming 30 000 nephrons per kidney). The capacity of the PTC lysosomal pathway in healthy rats has previously been demonstrated to be much lower at ~ 0.13 g/rat/day.^{3,20} We speculate that this is consistent with the low capacity binding site identified by Park and Maack²⁸ whereas post-glomerular uptake and retrieval of albumin, which will be ~ 2 g/rat/day, is identified with their high-capacity binding site. The maximum uptake

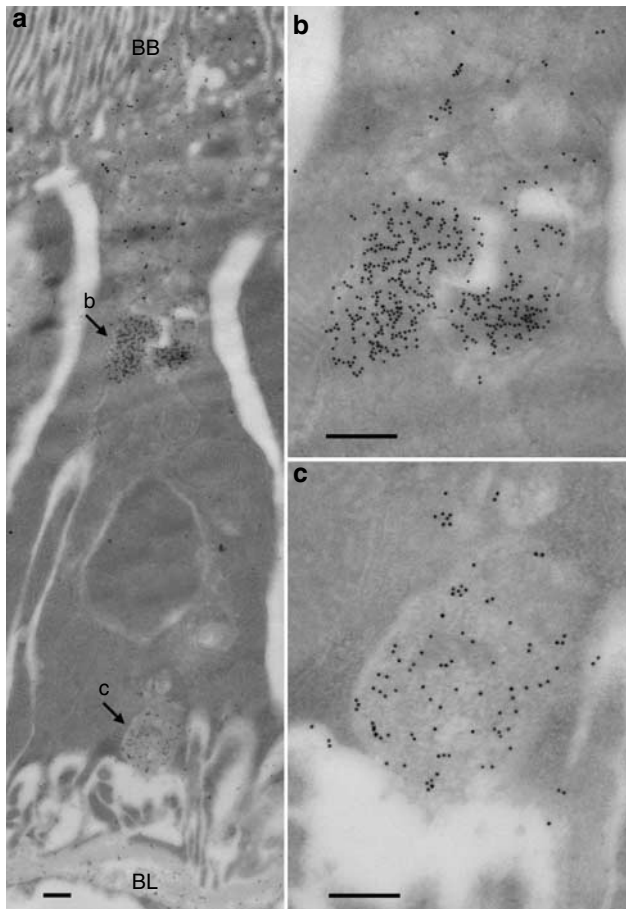


Figure 4 | Electron microscopy analysis of the distribution of endogenous albumin in renal PTCs. Before removal, the kidney was decapsulated, the ureter tied off and the renal artery and renal vein was clamped and the kidney was immediately removed and fixed by immersion fixation in paraformaldehyde lysine periodate (similar distribution for albumin was also seen when the ureter was not tied off). The kidney was processed for EM examination (see Materials and Methods) and immunogold labeling was carried out for RSA (10 nm gold) and megalin (15 nm gold). (a) Endogenous albumin is distributed through out the cell. Megalin (although not clearly seen at this magnification) is only observed in the upper most portion of the cell and presumably undergoes recycling to the apical membrane whilst the albumin is packed into larger vesicles (virtually devoid of megalin). (b) Enlarged view of the albumin laden vesicles presumed to undergo transcytosis toward the basolateral membrane. (c) Enlarged view of a vesicle laden with albumin discharging its contents into the basolateral space. BB – brush border. BL – basolateral. Arrows indicate the location of images enlarged in (b) and (c). Bar = 100 nm.

efficiency of this site is at an albumin concentration ~ 1 mg/ml which corresponds to the initial filtrate concentrations measured in this study. The lysosomal degradation pathway and the retrieval pathway clearly provide two distinct pathways for the processing of albumin and their dysfunction may give rise to two distinct types of albuminuria particularly in terms of the level of albumin excretion rate.²⁰

Why are these GSCs so high as compared to those determined by micropuncture, which have been universally accepted in nephrology, and are >50 -fold lower? The most

recent micropuncture measurements of Tojo and Endou² are considered by many to be the most accurate estimation of albumin in the Bowman's space. They collected four fluid fractions at each site along the tubule lumen. The first fraction contained very high quantities of albumin (comparable to amounts measured in this study) with the other three fractions containing progressively less albumin. The data from the first three fractions was eliminated because of supposed extratubular contamination of albumin and it was assumed that the fourth was uncontaminated ultimately obtaining a GSC of 0.00062. As the method of each collection involves slowing tubular flow by injecting oil into the tubule distally it means that at each collection site the albumin content in the lumen will be time dependent as the retrieval pathway will be continually removing albumin from the immobile fluid. The low levels of albumin seen in the fourth fraction collected at each site could then be owing to endocytosis of albumin from the stagnant filtrate that occurred during the collection of the first three fractions. Earlier reports had also remarked on albumin contamination from micropuncture fluid samples.²⁹

How can the high GSC be reconciled with the concept that the glomerular slit diaphragm is a 'limiting barrier' for albumin particularly when specific structural changes (often genetically induced) in the slit diaphragm may cause proteinuria? Although the normal slit diaphragm may be limiting in terms of size selectivity it is still allowing nephrotic levels of albumin to be transported through it. Any changes in the slit diaphragm may increase that albumin flux through changes in size selectivity (although these have yet to be measured in altered genetic states). Significant changes in glomerular permeability would be required in prolonged nephrotic states (where albumin flux is less owing to hypoalbuminemia) so that the retrieval pathway is approaching saturation and the excess unretrieved albumin is excreted.

We demonstrate in this study that the GSC for albumin in untreated controls is essentially the same as the fractional clearance of albumin in PAN rats.^{3,11,12} Changes in the albumin GSC in PAN rats cannot be eliminated but previous studies have demonstrated that for molecules of the same size as albumin glomerular permeability is not altered in PAN.^{3,11} The major difference is that in the untreated controls albumin is rescued back to the blood preventing excretion. Assuming the glomerular filtration rate is reduced by 40%^{12,13} in PAN rats and their plasma albumin reduced by two-thirds^{12,13} the predicted albumin excretion rate would be ~ 400 mg/day, which is close to that observed previously.^{12,13} This means that inhibition of PTC uptake is near $>80\%$. This has been established in this study using 2-photon microscopic analysis and the observation of reduced expression of endocytotic proteins in PAN rats. Other studies have demonstrated that specific inhibitors of these endocytotic proteins cause albuminuria.²⁶

In summary the significant uptake of albumin and suggested transcytosis of albumin by PTCs as demonstrated

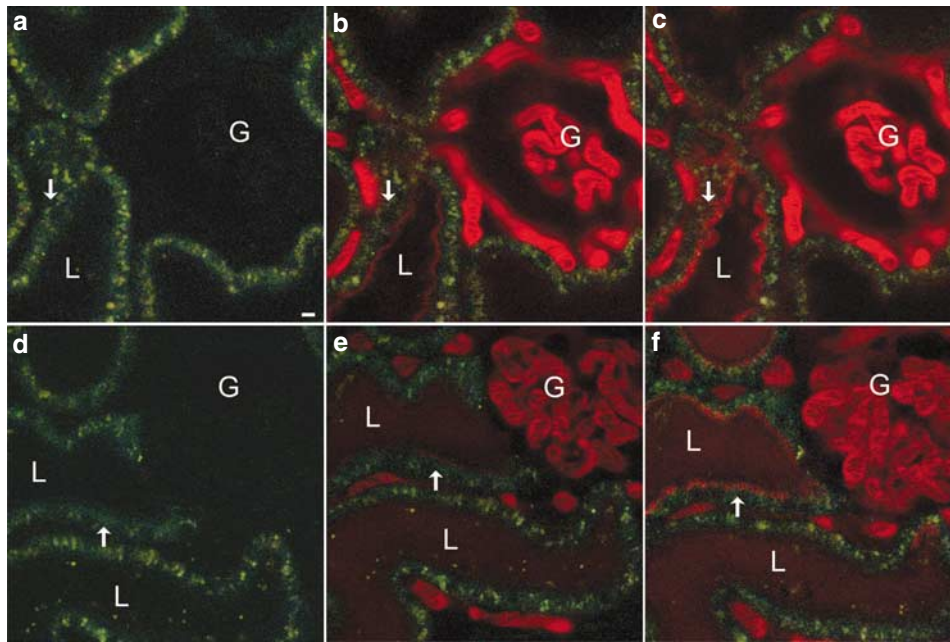


Figure 5 | Comparison of Alexa 568-RSA uptake of untreated and PAN nephrotic rats. As the PAN rat is hypoalbuminemic, the concentrations of fluorescent-labeled albumin were adjusted so that the ratio of labeled albumin to unlabeled endogenous albumin were essentially the same for untreated non-nephrotic rats and PAN rats. Distribution of Alexa 568-RSA in control rats injected with Alexa 568-RSA at (a) 0 s, (b) 40 s, and (c) 14 min. The arrows indicate a region where there is increasing amounts of labeled albumin seen. PAN rats injected with Alexa 568-RSA at (d) 0 s, (e) 40 s, and (f) 14 min. Arrows indicate a dark region where the brush border remains devoid of albumin. It is apparent that the uptake of albumin by the brush border is considerably reduced in the nephrotic rat. See Movies S5 and S6. Bar = 10 μ m.

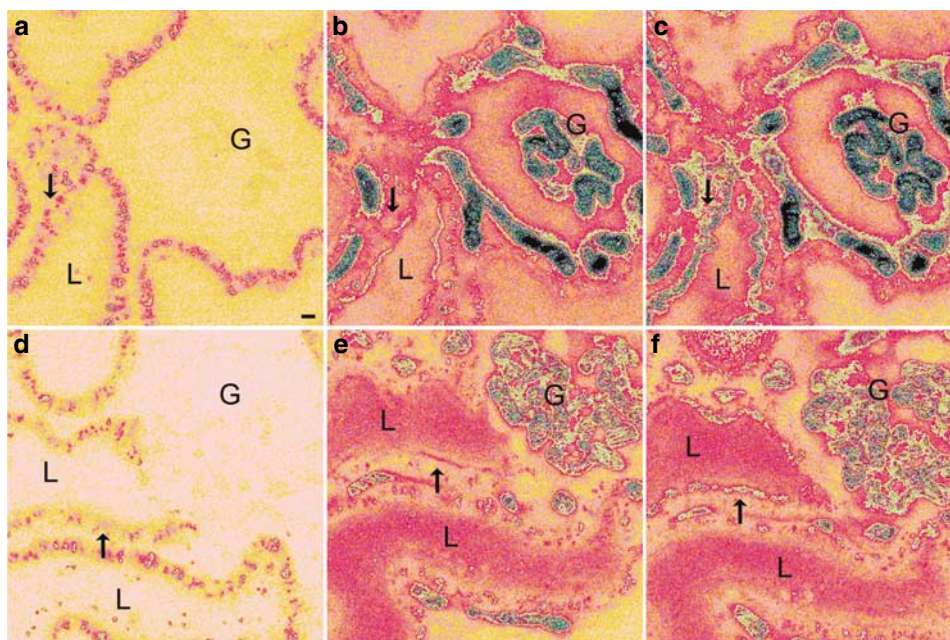


Figure 6 | Pseudocolor representation of the images in Figure 5 of Alexa 568-RSA uptake in control and nephrotic rats. It is apparent that there are markedly different distributions of the relatively low levels of albumin seen as the pink color. In the control rats finite levels of albumin are seen in the tubular lumen but also as a haze (see arrows) within the cytoplasm of the PTCs that extends to the basolateral side of the cell. Conversely, in PAN rats most of the albumin is seen in the tubular lumen with little uptake (see arrows) in the cytoplasm of the PTCs. Pseudocolor representation of the distribution of Alexa 568-RSA in control rats at (a) 0 s, (b) 40 s, and (c) 14 min. The arrows indicate a region where there is increasing amounts of labeled albumin seen. Pseudocolor representation of PAN rat kidney distribution of injected Alexa 568-RSA at (d) 0 s, (e) 40 s, and (f) 14 min. Bar = 10 μ m.

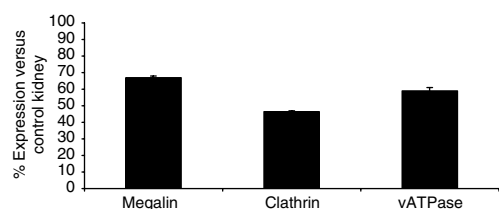


Figure 7 | Decreased expression of megalin, clathrin, and v-ATPase in rat nephrotic PTs. Immunocytochemistry of proteins regulating albumin endocytosis in the proximal tubular cell. $N = 3$ for rat control and PAN rat samples. Results presented as % of control apical protein expression intensity (mean \pm s.e.m.). For all points $P < 0.001$ versus their respective controls.

by 2-photon microscopy as well as by electron microscopy is consistent with high capacity handling of albumin in rats. These findings present a paradigm shift in the understanding of the etiology of albuminuria – that is, nephrotic levels of albumin are normally filtered across the glomerular capillary wall and albuminuria can result if there is inhibition of the retrieval process. The leakage of albumin and its subsequent retrieval explains the anticlogging properties for the high fluid flow glomerular filter. Further, the retrieval pathway appears to be a sorting mechanism for detecting structurally altered plasma albumin which is disposed of by the degradation pathway.¹⁸ These results provide a breakthrough in our understanding of renal physiology and the renal processing of albumin as well as providing important information regarding the mechanism of albuminuria.

MATERIALS AND METHODS

Animals

Guidelines and protocols established by the IACUC were strictly followed. Normal male Munich–Wistar rats weighing 150–200 g were used. Rats were allowed free access to water and standard rat chow. Albumin excretion rate measured by the Bradford assay over 24 h for Munich–Wistar rats ($n = 2$) was normal (10.9 mg/24 h). Nagase analbuminemic rats were obtained from a colony maintained by Professor George Kaysen at University of California Davis. Rats were anaesthetized by intraperitoneal injection of 45 mg/kg body weight of pentobarbital sodium (Abbott Laboratories, Chicago, IL, USA) (for all kidney fixation experiments) or by Halothane inhalation (2-photon microscopy). During 2-photon microscopy experiments body temperature was monitored using a rectal thermometer and maintained using a homeothermic table.

Probes and protein labeling

Rhodamine-dextran (40 kDa) was purchased from Molecular Probes (Eugene, OR, USA). Fluorescein isothiocyanate-inulin was from Sigma (St Louis, MO, USA). RSA fraction V (Sigma) was labeled with Alexa fluorophores Alexa 488 and Alexa 568 (Molecular Probes) using the supplier's method. Sodium dodecyl sulfate-polyacrylamide gel electrophoresis revealed that the labeled albumin cobanded with the unlabeled albumin standard. Size exclusion analysis of Alexa 568-RSA on PD10 columns (Pharmacia Fine Chemicals, Uppsala, Sweden) revealed that there was no low-molecular weight contamination of the labeled preparation ($< 0.3\%$) (not shown). Stock solutions of rhodamine-dextran

and Alexa albumins were at approximately 20 and 17 mg/ml, respectively. A 20 mg/ml solution of fluorescein isothiocyanate-inulin in 0.9% saline was dialyzed against 1000 MW cutoff membrane. The final concentration was 16.6 mg/ml. Quality control studies demonstrated that the plasma clearance rate measured¹³ over 24 h of Alexa 568-RSA was $0.023 \pm 0.001 \text{ h}^{-1}$ ($n = 3$ in 300 g Sprague–Dawley rats) which is similar to that obtained previously for tritium-labeled albumin in healthy rats ($0.019 \pm 0.003 \text{ h}^{-1}$) as compared to PAN rats ($0.050 \pm 0.011 \text{ h}^{-1}$).¹³ Furthermore, the fractional clearance of Alexa 568-RSA was similar to albumin as studied in the isolated perfused kidney¹⁷ system (data not shown).

2-photon microscopy

All imaging was conducted using a Bio-Rad MRC-1024MP 2-photon laser scanning microscope (Hercules, CA, USA) mounted on a Nikon Diaphot inverted stage platform (Fryer, Huntley, IL, USA) utilizing a Ti:Sapphire laser (Spectra-Physics, Franklin, MA, USA) as described previously.^{9,10}

Image processing

Raw data collected were analyzed, quantified, and displayed using Metamorph v6.1 (Universal Imaging/Molecular Devices, Downingtown, PA, USA). The depth of field was 10–20 μm . The aoi were outlined and average fluorescence intensities were generated and reported after background subtraction. To quantify changes in intensity that occur between the tubular lumen, brush border, and cytosol, the line tool was used to draw a line across all three regions and quantified using the linescan function. Data are presented with intensity on the y axis and pixel number progression on the x axis with pixel No. 1 located in the capillary or cytoplasm of the cell and later pixels progressing to the tubular lumen. Finally, some images were presented using a pseudocolor palette to help distinguish subtle changes in fluorescence intensity, particularly at the lower intensities inherent to the albumin concentration in the PT cytosol. This palette replaces gray scale with a color scale ranging from magenta to light green to turquoise to black for dim to bright intensities, respectively.

GSC estimates

Bolus injection. Glomeruli with attached SI segment were chosen at random and imaged. Fluorescent probes were dissolved in isotonic saline and injected into the femoral vein or jugular vein of anaesthetized rats in a steady bolus of 0.2–0.4 ml over 5 s. GSC estimates were made of the ratio of labeled material in the plasma and labeled material at the center of the interface of the S1 tubular lumen with the Bowman's capsule (Figure 1). In all cases we observed rapid and continuous perfusion of the glomerulus during the experiment. In some experiments, serum fluorescence at saturating levels ($> 220 \text{ U}$) was analyzed by diluting the serum (collected at regular intervals from the tail vein during the course of the experiment) and using the 2-photon microscope under the same objective used for the *in vivo* imaging. The linear standard curve obtained allowed us to obtain quantitative values in the lumen and regions on the brush border. The linear range of fluorescence extended from 0 to 220 U. Studies have shown that non-saturating levels of plasma fluorescence were essentially identical to that measured in glomerular capillaries directly (four measurements made on blood plasma *in vitro* gave a mean of 197 U whereas direct *in vivo* measurement in the glomerular capillary gave a value of 189 U).

Steady-state levels of plasma-labeled albumin and inulin.

Inulin was initially injected intravenously via the jugular vein as a bolus of 2 mg/ml in 400 μ l followed by steady infusion of 16.6 mg/ml at 37 μ l/min. Albumin was initially injected as a bolus of 6.4 mg/ml in 400 μ l followed by steady infusion of 43 μ g/ml at 50 μ l/min. For inulin 120 s videos were recorded every 4 min over a 20-min period. For albumin 90 s videos were recorded every 4–5 min over a 30-min period. GSC was quantified as described in the previous section.

Induction of PAN. Male Munich–Wistar rats were injected intravenously with 15 mg/100 g body weight puromycin aminonucleoside given as a 3.5% solution in phosphate-buffered saline (PBS) (pH 7.4) via the tail vein as described previously.^{11,12} Eight days after PAN induction, animals were assessed by 2-photon microscopy or kidneys were fixed for immunocytochemistry by perfusion with 4% paraformaldehyde lysine periodate and sectioned as described previously for immunocytochemical analysis.³⁰

Immunocytochemical staining

Kidney sections from PAN and control rats were re-hydrated in PBS for 5–10 min and blocked using a 1% casein in PBS (for albumin staining) or treated for 4 min in 1% sodium dodecyl sulfate and blocked with 1% bovine serum albumin in PBS (megalin, clathrin, and v-ATPase staining). Primary antibodies used were: megalin monoclonal antibody (1:600 dilution) (generous gift from Dr Robert McCluskey) previously characterized,³¹ monoclonal clathrin heavy chain (BD Transduction Laboratories, San Jose, CA, USA) (1:100 dilution), and polyclonal v-ATPase (1:600 dilution) 70 kDa A subunit antibody raised against the last 10 amino acids (CMQNAFRSLE) of the c-terminal tail of the v-ATPase A subunit. Secondary antibodies used were goat anti rabbit IgG-CY3 (1:800 dilution), goat anti rabbit fluorescein isothiocyanate IgG (1:600 dilution) and donkey anti mouse IgG-CY3 (1:800 dilution) (Jackson ImmunoResearch Laboratories, PA, USA).

Electron microscopy and immunogold staining

Rats were anaesthetized and the right-hand side kidney was gently decapsulated, the ureter tied off, and the renal artery and renal vein clamped (to prevent blood loss from the kidney), the whole kidney was then immediately removed and immersion fixed in paraformaldehyde lysine periodate. It should be noted that the same distributions of albumin in PT cells was observed in a similar procedure where the ureter was not tied off. For electron microscopy immunogold staining, small pieces of paraformaldehyde lysine periodate immersion-fixed rat kidney (less than 1 mm³) were dehydrated through a graded series of ethanol to 100% ethanol. They were then infiltrated with LR White resin (Electron Microscopy Sciences, Fort Washington, PA, USA) and were placed in fresh LR White for a few hours and embedded in gelatin capsules at 50°C overnight. For the immunostaining, thin sections were cut on a Reichert Ultracut E ultramicrotome and were collected on formvar-coated nickel grids. The grids were incubated on drops of 1% bovine serum albumin/PBS + 5% normal goat serum (Sigma) for 10 min at room temperature as a blocking step. They were then placed on drops of either DAKO antibody diluent (negative control, DAKO Corp., Carpinteria, CA, USA), or on drops of primary antibody diluted in DAKO diluent (polyclonal anti-RSA (ICN pharmaceuticals Aurora, OH, USA) 1:20 dilution or megalin monoclonal antibody 1:100 dilution) for 1 h, at room temperature. Following

several rinses on drops of PBS, the grids were incubated on drops of gold-conjugated secondary antibody (1:20 dilution) (Ted Pella, Inc., Redding, CA, USA) for 1 h at room temperature. Finally, the grids were rinsed several times on drops of distilled water and stained for 5 min on drops of aqueous uranyl acetate electron microscopy sciences (EMS). They were rinsed on drops of distilled water, dried, and examined in a JEOL 1011 transmission electron microscope at 80 kV.

Quantification of immunofluorescence staining intensity

For quantification, digital images were acquired in a blinded manner using a Nikon fluorescence microscope (equipped with a Hamamatsu Orca CCD camera) with a $\times 20$ objective. Images from each group were collected with the same microscope setting. PTs were chosen at random and an aoi was drawn around the apical pole and analyzed on a Macintosh computer using IP Lab Spectrum acquisition and image analysis software. Values were automatically recorded in a spreadsheet and statistically compared using Microsoft Excel software. Six pictures were taken from each of three samples and five PTs were independently analyzed from each picture (a total of 90 PTs analyzed for each rat group).

ACKNOWLEDGMENTS

We gratefully thank Dr Silvia B Campos for her excellent technical assistance. These studies were supported by a R&D grant to WD Comper by AusAm Biotechnologies; an NIH Grant DK 061594 awarded to BA Molitoris to establish a George M O'Brien Center for Advanced Renal Microscopic Analysis at the Indiana Center for Biological Microscopy, and NIH Grant DK 42956 to D Brown. LM Russo is the recipient of a Postdoctoral and an Advanced Postdoctoral Fellowship Award from the Juvenile Diabetes Research Foundation. Preliminary parts of this work were presented as posters at the 37th and 38th Annual meeting of the American Society of Nephrology.

SUPPLEMENTARY MATERIAL

Movie S1. Once the glomerulus in the right-hand corner is flushed with albumin one can visualize the uptake of albumin over a very long tubular lumen.

Movie S2. The silhouette of the brush border is clearly evident in the pre-injection images of the nagase analbuminemic rats.

Movie S3. The infusion of green albumin and red dextran.

Movie S4. The distribution of green albumin 38 min after its infusion.

Movie S5. PAN rats reveal observable quantities of albumin in the tubular lumen but very little uptake by the brush border.

Movie S6. The lack of albumin uptake into the proximal tubular cell is evident in the PAN rat 13 min after infusion of the albumin.

Figure S1. Representative immunocytochemistry pictures demonstrating that megalin, v-ATPase, and clathrin expression is reduced in PAN nephrotic rat kidney.

REFERENCES

1. Tryggvason K, Wartiovaara J. Molecular basis of glomerular permselectivity. *Curr Opin Nephrol Hypertens* 2001; **10**: 543–549.
2. Tojo A, Endou H. Intrarenal handling of proteins in rats using fractional micropuncture technique. *Am J Physiol* 1992; **263**: F601–F606.
3. Greive KA, Nikolic-Paterson DJ, Guimarães MAM *et al*. Glomerular permselectivity factors are not responsible for the increase in fractional clearance of albumin in rat glomerulonephritis. *Am J Pathol* 2001; **159**: 1159–1170.
4. Guimarães MAM, Nikolovski J, Pratt LM *et al*. Anomalous fractional clearance of negatively charged Ficoll relative to uncharged Ficoll. *Am J Physiol* 2003; **285**: F1118–F1124.
5. Schaeffer Jr RC, Gratrix ML, Mucha DR, Carbajal JM. The rat glomerular filtration barrier does not show negative charge selectivity. *Microcirculation* 2002; **9**: 329–342.

6. Vyas SV, Burne MJ, Pratt LM, Comper WD. Glomerular processing of dextran sulphate. *Arch Biochem Biophys* 1996; **332**: 205–212.
7. Asgeirsson D, Rippe B, Venturoli D, Rippe C. Increased glomerular permeability to negatively charged Ficoll relative to neutral Ficoll in rats. *Am J Physiol Renal Physiol* 2006; **291**: F1083–F1089.
8. Yu W, Sandoval RM, Molitoris BA. Quantitative intravital microscopy using a generalized polarity concept for kidney studies. *Am J Physiol* 2005; **289**: C1197–C1208.
9. Dunn KW, Sandoval RM, Kelly KJ *et al.* Functional studies of the kidney of living animals using multicolor two-photon microscopy. *Am J Physiol* 2002; **283**: C905–C916.
10. Sandoval RM, Kennedy MD, Low PS. Uptake and trafficking of fluorescent conjugates of folic acid in the intact kidney using intravital 2-photon microscopy. *Am J Physiol* 2004; **287**: C517–C526.
11. Osicka TM, Strong KJ, Nikolic-Paterson DJ *et al.* Renal processing of serum proteins in an albumin-deficient environment: an *in vivo* study of glomerulonephritis in the Nagase albuminaemic rat. *Nephrol Dial Transplant* 2004; **19**: 320–328.
12. Osicka TM, Hankin AR, Comper WD. Puromycin aminonucleoside nephrosis results in a marked increase in fractional clearance of albumin. *Am J Physiol* 1999; **277**: F139–F145.
13. Koltun M, Nikolovski J, Strong K *et al.* Mechanism of hypoalbuminemia in rodents. *Am J Physiol* 2005; **288**: H1604–H1610.
14. Eppel GA, Osicka TM, Pratt LM *et al.* The return of glomerular filtered albumin to the rat renal vein. *Kidney Int* 1999; **55**: 1861–1870.
15. Gudehithlu KP, Pegoraro AA, Dunea G *et al.* Degradation of albumin by the renal proximal tubule cells and the subsequent fate of its fragments. *Kidney Int* 2004; **65**: 2113–2122.
16. Blouch K, Deen WM, Fauvel JP *et al.* Molecular configuration and glomerular size selectivity in healthy and nephrotic humans. *Am J Physiol* 1997; **273**: 430–437.
17. Osicka TM, Pratt LM, Comper WD. Glomerular capillary wall permeability to albumin and horseradish peroxidase. *Nephrology* 1996; **2**: 199–212.
18. Clavant SP, Comper WD. Urinary clearance of albumin is critically determined by its tertiary structure. *J Lab Clin Med* 2003; **142**: 372–384.
19. Koltun M, Comper WD. Retention of albumin in the circulation is governed by saturable renal cell-mediated processes. *Microcirculation* 2004; **11**: 351–360.
20. Russo LM, Bakris G, Comper WD. Renal handling of albumin. A critical review of basic concepts and perspective. *Am J Kidney Dis* 2002; **39**: 899–919.
21. Tencer J, Frick IM, Oquist BW *et al.* Size-selectivity of the glomerular barrier to high molecular weight proteins: upper size limitations of shunt pathways. *Kidney Int* 1998; **53**: 709–715.
22. Ohno Y, Birn H, Christensen EI. *In vivo* confocal laser scanning microscopy and micropuncture in intact rat. *Nephron Exp Nephrol* 2005; **99**: e17–e25.
23. Birn H, Fyfe JC, Jacobsen C *et al.* Cubilin is an albumin binding protein important for renal tubular albumin reabsorption. *J Clin Invest* 2000; **105**: 1353–1361.
24. Cui S, Verroust PJ, Moestrup SK, Christensen EI. Megalin/gp330 mediates uptake of albumin in renal proximal tubule. *Am J Physiol* 1996; **271**: F900–F907.
25. Birn H, Christensen EI. Renal albumin absorption in physiology and pathology. *Kidney Int* 2006; **69**: 440–449.
26. Hilliard LM, Osicka TM, Robinson PJ *et al.* Characterisation of the urinary albumin degradation pathway in the isolated perfused rat kidney. *J Lab Clin Med* 2006; **147**: 36–44.
27. Hurtado-Lorenzo A, Skinner M, El Annan J *et al.* V-ATPase interacts with ARNO and Arf6 in early endosomes and regulates the protein degradative pathway. *Nat Cell Biol* 2006; **8**: 124–136.
28. Park CH, Maack T. Albumin absorption and catabolism by isolated perfused proximal convoluted tubules of the rabbit. *J Clin Invest* 1992; **73**: 767–777.
29. Oken DE, Flamebaum W. Micropuncture studies of proximal tubule albumin concentration in normal and nephrotic rats. *J Clin Invest* 1971; **50**: 1498–1505.
30. Beaulieu V, Da Silva N, Pastor-Soler N *et al.* Modulation of the actin cytoskeleton via gelsolin regulates vacuolar H⁺-VATPase recycling. *J Biol Chem* 2005; **280**: 8452–8463.
31. Marino M, Andrews D, Brown D, McCluskey RT. Transcytosis of retinol-binding protein across renal proximal tubule cells after megalin (gp 330)-mediated endocytosis. *J Am Soc Nephrol* 2001; **12**: 637–648.